

OPTICAL CHARACTERIZATION OF STABILIZED ATMOSPHERIC PRESSURE PIN TO PLATE PLASMA SOURCE

Ahmed Abdelradi ^{a,*}, Ahmed Samir ^b, Farouk Elakshar ^c, Abdou Garamoon ^c, Mansour ElSabbagh ^{b,c}

^a Egyptian Meteorological Authority, Cairo, Egypt.

^b Center of Plasma Technology, Al-Azhar University, Cairo, Egypt

^c Department of Physics, Faculty of Science, Al-Azhar University, Cairo, Egypt.

*Corresponding author: ah_ph_86@yahoo.com.

Received: 24 Aug 2021; Revised: 23 Sep 2021; Accepted: 01 Oct 2021; Published: 01 Dec 2021

ABSTRACT

DC Stabilized Discharges (DCSD) was generated in atmospheric pressure argon for a pin to plate. In this paper, discharge with a flowing argon gas into the air (plasma Source) is investigated by optical emission spectroscopy technique. The emission spectra of excited species of atomic-hydrogen, N₂ and Ar were observed and measured. The rotational and vibrational temperatures of the discharge were measured by comparing modelled optical emission spectra with measured spectra from the discharge by using several different vibrational bands of the 2nd positive system (SPS) of N₂ (N₂[C ³Π_u] → N₂[B ³Π_g]). The optical characteristics of the discharge shown that the DCSD was found to be non-equilibrium with rotational temperature (T_r) of 1087 K and vibrational temperature (T_v) of 1661 K. Boltzmann plot method has been applied to estimate the electronic excitation temperature which was found to be 1.36 eV and 1.1 eV for discharges with argon flow rates of 1.0 SLM & 0.5 SLM respectively. This finding proved the strong non-equilibrium nature of the discharge conditions of the current work.

Keywords: Atmospheric Pressure; Pin to Plate; Stabilized

1. INTRODUCTION

Over the last two decades, research on atmospheric pressure non-equilibrium plasmas has intensified, resulting in a wide range of plasma sources for a wide range of applications such as chemical conversion, medicine, chemical analysis, and disinfection., without the need for vacuum equipment. Non-thermal plasma (also known as a cold plasma or non-equilibrium plasma) are typically characterized by their translational temperature (T_{trans}) < rotational temperature (T_{rot}) < vibrational temperature (T_{vib}) < electron temperature (T_e) [1-2]. In plasma-assisted materials applications,

Available at Egyptian Knowledge Bank (EKB)

the nonequilibrium nature enables active species to interact with the sample without generating too much heat which could destroy the sample [3-5]. Non-equilibrium plasma is a future tool for the treatment of cancer, some diseases, and many medical applications [6-9].

Although non-equilibrium glow discharges at low pressure can be easily produced (usually a few hundred Volts DC), the glow discharge tends to be unstable and restricted with rising pressure: a glow-to-spark transition occurs. Special geometries, electrodes, or excitation methods should therefore be used to create

Journal Homepage: <https://absb.journals.ekb>

glow discharges at atmospheric pressure [10-12].

Non-equilibrium atmospheric pressure glow discharges have to be stabilized with disparate solutions, Take, for instance, by connecting a resistor in series. For constant applied voltage, the series resistor can prevent current runaway by causing the voltage across the discharge gap to decrease with increasing current. A capacitor or inductance in series with the discharge gap can produce similar results. The latter has been shown by Aldea *et al.* [13], who used it to stabilize large area APGDs for material treatment applications. Atmospheric pressure glow discharges stabilized by resistive electrodes are studied by Laroussi *et al.* [14]. Also, water is used to generate glow discharges, as has been studied by Andre *et al.* [15], Lu and Laroussi [16], and Bruggeman *et al.* [17]. Staack *et al.* [18] examined DC glow and micro glow discharges between two metal electrodes. Because of the high surface–volume ratio and consequently efficient heat disposal, the micro glow discharges remain stable. Akishev and Leys groups studied how to keep high-current glow discharges stable. The transition from the glow to the spark can be postponed to bigger currents with a gas flow on the order of 10 ms^{-1} [19, 20]. Staack *et al.* [21], found that the ionization overheating instability leading to transition of the discharge to the contracted state, In order to prevent developing of instabilities of glow discharge in transverse gas flow the partitioned cooled cathodic blocks are used by cathodic sections in the cathodic block are separated from each other by dielectric layers.

In the current work we constructed pin to plate plasma source operating at atmospheric pressure to generate stabilized non-equilibrium plasma for material processing applications. We investigated the produced plasma using optical emission spectroscopy. The strategy of obtaining stabilized atmospheric pressure non-equilibrium plasma was to remove the

produced heat the discharge region by flowing argon through the needle electrode in addition to using a massive stainless steel cathode.

This paper is organized as follows. After this general introduction, Section 2 describes the experimental setup used for creating and analysing the pin to plate. Results and discussion is presented in section 3 while the conclusion of the work is presented in section 4.

2. EXPERIMENTAL SETUP

The arrangement for creating and analysing data of stabilized discharge is depicted in figure 1 and a photograph of the discharge is shown in figure 2. We used a stainless steel needle as an anode with a 0.5 mm inner diameter. Working argon gas was fed through the needle anode, which was placed above a stainless-steel plate working as cathode with a separation distance of 3.4 mm in the open air. The gas flow rate was adjusted in the range from 0.20 to 2.0 SLM with the use of a mass flow controller (MC-2SLPM-D/5 M, Alicat Scientific), which is connected in parallel with the anode through a rubber tube and the setup's ground was connected to the cathode. A homemade DC power source was constructed and utilised to derive the discharge. This power supply is capable of deriving the discharge by applying an applied voltage up to 12 kV and current 50mA. The discharge current was limited by a $100 \text{ k } \Omega$ load resistance. The cathode plate was connected to the ground potential via a 100Ω resistor to measure the discharge current which is equal to the potential drop across the resistor divided by the resistor value. A home-made voltage probe was used to measure the discharge voltage, which was linked in parallel with the needle anode and the setup's ground.

A UV–VIS SD2000 dual fibre optic emission spectrometer from Ocean optics was used to monitor the optical emission spectroscopy (OES) at the centre of the discharge region.

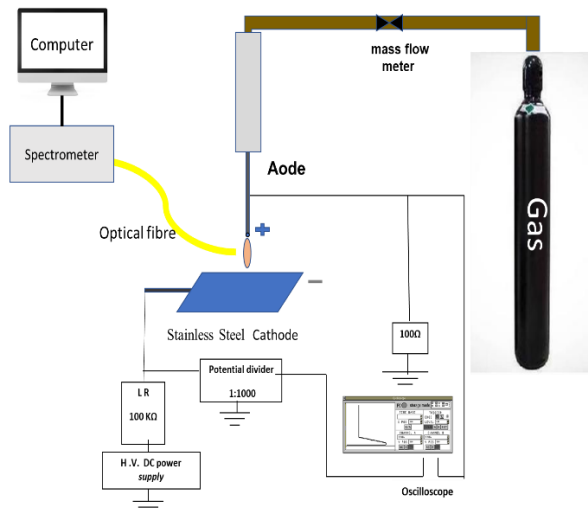


Fig. 1. The electrical circuit that is used to generate DCSD.

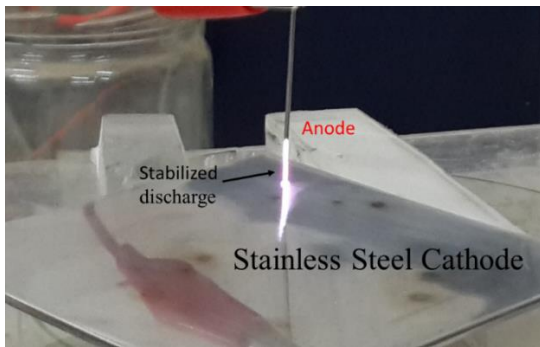


Fig. 2. Photograph of DCSD.

3. RESULTS AND DISCUSSION

DCSD was studied using optical emission spectroscopy at atmospheric pressure needle anode to plate cathode discharge where argon gas was flowing through the needle anode into air. All spectra were measured for emission collected from the centre of the discharge where the separation distance of the anode and the cathode was set at 3.4 mm. The emitted spectra were analysed to identify the reactive species in the discharge. Emission of some of argon atomic and ionic lines was used to define the electronic excitation temperature of DCSD using Boltzmann plot method. The rotational and vibrational temperatures (T_r & T_v) of the N_2 second positive system ($C^3\Pi_u - B^3\Pi_g$ transition) were evaluated by comparing the experimental observations with simulated spectra.

3.1. Identification of species in the discharge region

Optical emission spectra of the discharge operated with argon flow rates of 0.5 and 1.0 SLM for discharge current of 30 mA (standard litre per minute) were analysed to identify the species that generated in the discharge region. Optical emission spectra can be divided into three regions. UV region for emission below 400 nm, visible region for emission between 400 nm to 700 nm and infrared region for emission above 700 nm.

a) UV Region

Emission spectra in the UV region are depicted in figures 3(a) and 3(b) for discharge of argon flow rates of 0.5 SLM & 1.0 SLM respectively. The N_2 Second Positive System is responsible for the most powerful emissions recorded between 350 and 400 nm ($N_2[C^3\Pi_u] \rightarrow N_2[B^3\Pi_g]$) emission bands, with a prevailing emission (0,1) band head at 357.69 nm, emission (0,2) band head at 380.49 nm, emission (1,3) band head at 375.5 nm, emission (1,2) band head at 353.83 nm. In addition to few weak argon ionic lines. The N_2 Second Positive System's emission ($N_2[C^3\Pi_u] \rightarrow N_2[B^3\Pi_g]$) is attributed to the nitrogen gas of the surrounded air that is entrained to the discharge region[28]. From figures 3(a) & 3(b) the N_2 Second Positive Emission Intensity for the discharge of argon flow rate of 1.0 SLM is weaker than that of the argon flow rate of 0.5 SLM case. This might be attributed to the smaller density of nitrogen gas entrained in the discharge region for the case of the argon flow rate of 1 SLM compared to that entrained for the argon flow rate of 0.5 SLM case.

b) Visible Region

Figures 4(a) and 4(b) exhibit emission spectra in the visible portion of the spectrum for argon flow rates of 0.5 SLM and 1.0 SLM, respectively. The N_2 Second Positive System ($N_2[C^3\Pi_u] \rightarrow N_2[B^3\Pi_g]$) emission (0,3) band head at 405.94 nm was observed in addition to the second-order (0,0) band at 674.13 nm. Atomic hydrogen lines H_β and H_α were observed at 486.13 nm and 656.3 nm

respectively, where H_β intensity is much weaker than H_α . The origin of the atomic hydrogen emission might be ascribed to the hydrogen gas in the discharge region because of the dissociation of water vapour which entrained in the discharge region as can be seen from the following reactions [29-34].

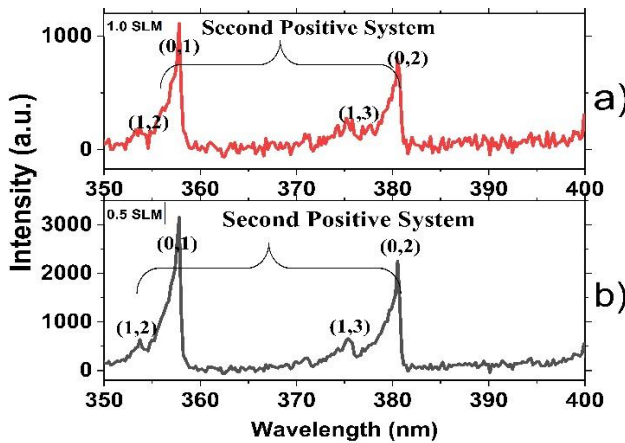
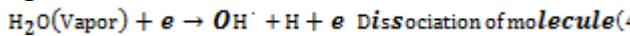
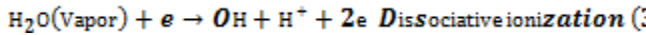
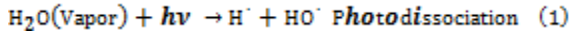


Fig. 3. Spectra of emission of DCSD in UV region
Gap: 3.4 mm; $I = 30$ mA.

- (a) Flowrate 1.0 SLM and accumulation times=30 ms
(b) Flowrate 0.5 SLM and accumulation times=30 ms

Several atomic and ionic argon emission lines were also identified, which are belonged to the NIST database [35]. It should be mentioned here that all the emission intensities for the discharge with argon flow rate of 0.5 SLM are stronger than that for the discharge with argon flow rate. 1.0 SLM. This might be attributed to the smaller density of nitrogen gas entrained in the discharge region for the case of the argon flow rate of 1SLM compared to that entrained for the argon flow rate of 0.5 SLM case.

c) Near IR Region

The emission spectra of DCSD for argon between 700 and 1000 nm are shown in Figures 5(a) and 4(b) for discharges with argon flow rates of 0.5 SLM and 1.0 SLM, respectively. This region was rich with strong emission atomic argon lines which were listed in table 2. In addition, weak atomic oxygen lines at 777.41 nm and 844.6 nm were observed. It is clearly seen from figures 5(a) & 5(b) that the

emission intensity of atomic argon lines in this region for discharge with argon flow rate of 1.0 SLM is stronger than that for discharge with argon flow rate of 0.5 SLM. This might be attributed to the higher excitation temperature of 1.0 SLM flow rate compared with that of 0.5 SLM discharge conditions.

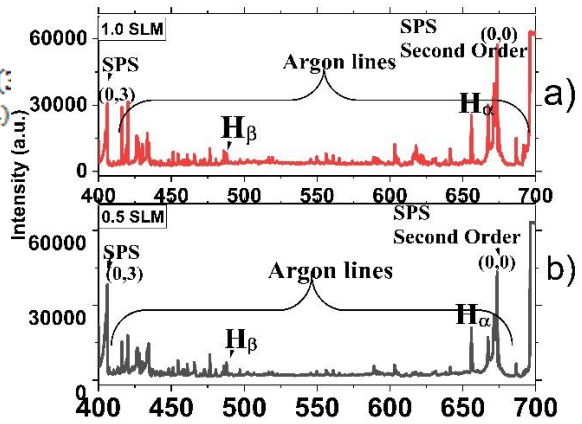


Fig. 4. Spectra of emission of DCSD in the visible region

Gap: 3.4 mm; $I = 30$ mA.

- Flowrate 1.0 SLM and accumulation times= 1s
Flowrate 0.5 SLM and accumulation times= 2s

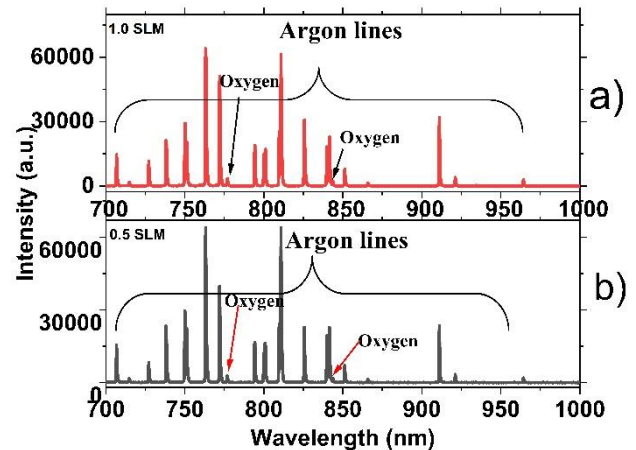


Fig. 5. Spectra of emission of DCSD Near IR region
Gap: 3.4 mm; $I = 30$ mA.

- (a) Flowrate 1.0 SLM and accumulation times=30 ms
(b) Flowrate 0.5 SLM and accumulation times= 30ms

3.2. Determination of Rotational and Vibrational Temperatures

The spectra of the N_2 2nd positive system N_2 [$\text{B } ^3\Pi_g$] released in the air are the most useful for plasma diagnostics because they allow for the determination of rotational T_r and

vibrational T_v temperatures by comparing experimental and simulated spectra [36]. To measure the rotational (T_r) and vibrational (T_v) temperatures of the plasma, we employed software created at the Technical University of Eindhoven [26]-[37]. Software is used to model the emission bands of the N_2 2nd positive system $N_2[B^3\Pi_g]$ with rotational-vibrational transitions at (0,1), (1,3), and (0,2) from 350 to 385 nm. Figure 6 shows an experimental spectrum of N_2 2nd positive system $N_2[B^3\Pi_g]$ bands emitted from the DCSD together with the simulated spectrum.

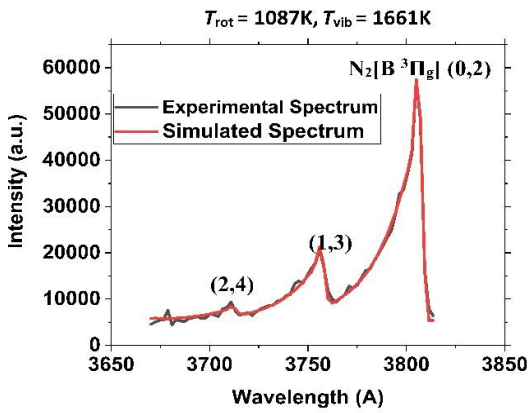


Fig. 6. Spectra measured and corresponding best fit modelled spectra

Gap: 3.4 mm; $I = 30$ mA.

Flowrate 1.0 SLM

With a correlation of 0.9975, the best fits of T_r and T_v temperatures were found to be 1087K and 1661K, respectively. The T_v and T_r values indicate that the discharge was non-equilibrium.

3.3. Electronic Excitation Temperature using Boltzmann Plot Method

The electronic excitation temperature T_{exct} is defined by fit a thermal distribution to the properly weighted intensities of a set of atomic and ionic transitions for a specific atomic and ionic species in the discharge. In the case of stabilized atmospheric pressure pin to plate plasma experiment, the atomic and ionic species used are atomic and ionic argon. The emitted atomic and ionic argon species are excited in the discharge and these species will emit spectra when they are de-excited. The

intensity I_{ij} of Ar I atomic and Ar ionic lines when Ar-atoms are de-excited from an initial excited state i to final state j is given by

$$I_{ij} = C_{ij} \cdot A_{ij} \cdot g_i \cdot \nu_{ij} \cdot \exp\left(\frac{-\epsilon_i}{T_{\text{exct}}}\right) \quad (5)$$

where C is proportionality constant, A_{ij} is atomic transition probability, g_i is statistical weight, ν_{ij} is frequency of the atomic or ionic line, and ϵ_i & T_{exct} are the energy of the level i and the excitation temperature in eV, respectively. Rearranging the previous equation, we get the following equation.

$$\frac{I_{ij} \cdot \lambda_{ij}}{A_{ij} \cdot g_i} = C \cdot \exp\left(\frac{-\epsilon_{\text{exct}}}{T_{\text{exct}}}\right) \quad (6)$$

where λ_{ij} is the wavelength of the emitted line. The plot of $\ln(I_{ij}\lambda_{ij}/A_{ij}g_i)$ as a function of ϵ_i for each of the selected emitted species, gives points that would be perfectly aligned in case of discharge in local thermal equilibrium (LTE). The slope of this line is $-1/T_{\text{exct}}$ leading to T_{exct} which is a good approximation for T_e in the case of LTE. This plot is called Boltzmann plot [38-45]. Each observed Ar atomic line wavelength has an associated energy level ϵ_i , a statistical weight g_i , and atomic transition probability A_{ij} as given in table 1. In our experiment, we get ϵ_i , g_i , and A_{ij} from the NIST Atomic Spectra Database [35].

Table1: Spectroscopic parameters of selected Ar emission spectral lines used to estimate plasma temperature using Boltzmann plot method at flowrate 0.5 SLM, 1.0 SLM, $I = 30$ mA that absorbed between the electrodes

Species	Wavelength (nm)	A_{ij} (s ⁻¹)	gk	E_j (eV)
Ar	415.86	1.40E+06	5	14.53
	420.07	9.67E+05	7	14.499
	446.05	1.50E+06	6	19.222
	451.07	1.18E+06	1	14.57
	454.5	4.71E+07	4	19.87
	460.96	7.89E+07	8	21.14
	465.79	8.92E+07	4	19.8
	475.29	4.50E+05	3	15.51
	476.45	6.40E+07	4	19.87
	487.62	7.80E+05	5	15.45
	487.98	8.23E+07	6	19.68
	430.065	5.70E+06	6	21.5
	421.86	3.60E+07	4	22.7
	422.69	4.10E+07	6	24.28
423.72	1.12E+07	4	21.35	

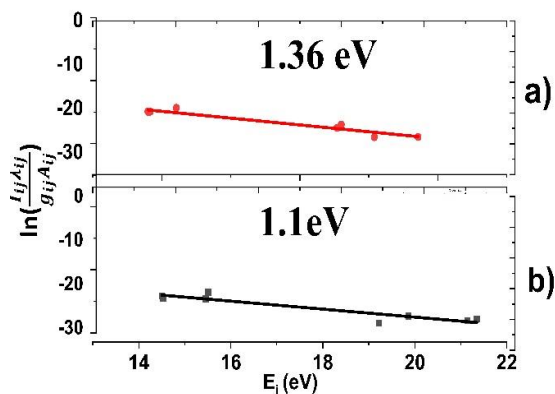


Fig. 7. Boltzmann distribution function plot of Ar emission spectral lines

Gap: 3.4 mm; I= 30 mA.

- (a) Flowrate 1.0 SLM and accumulation times=30 ms
 (b) Flowrate 0.5 SLM and accumulation times=30ms

Figures 7(a) and (b) show Boltzmann plots of argon discharge at flow rates of 0.5 SLM and 1.0 SLM, respectively. According to these results, the electronic excited temperature for discharge with argon flow rates of 0.5 SLM and 1.0 SLM is 1.1 eV and 1.36 eV, respectively. The data shown in figures 7(a) and 7 (b) are fitted by nice straight lines which ensure that the plasma in our discharge is followed local thermal equilibrium. The measured electronic excited temperature revealed that the discharge in the current work is strongly non-equilibrium.

CONCLUSION

This paper presents the experimental analysis of optical emission spectra for DC stabilized atmospheric plasma source. Identification of the discharge species revealed that the presence of nitrogen second positive system, atomic and ionic argon emission lines, atomic oxygen emission lines and atomic hydrogen emission lines. Rotational and vibrational temperatures were estimated by comparing the measured spectrum of the nitrogen second positive system with the simulated one. Boltzmann plot method was used successfully to determine the electronic excitation temperature. Rotational, vibrational

and electronic excitation temperatures proved that the discharge of the current work is strongly non-equilibrium. The finding of the current work, namely the non-equilibrium state of the discharge, ensure this plasma source is suitable for material processing applications which is the subject of the forthcoming publications.

Acknowledgements

This work has been made possible due to the generosity of the Science and Technology Development Fund (STDF), Egypt. Project ID: 22896.

REFERENCES

- [1] Staack D, Farouk B, Gutsol A F and Fridman A A . Spectroscopic studies and rotational and vibrational temperature measurements of atmospheric pressure normal glow plasma discharges in air. *Plasma Sources Science and Technology*. 2006; 15(4): 818–827. doi.org/10.1088/0963-0252/15/4/027
- [2] Staack D, Pollard W and Suzuki P. Striations in High-Pressure Hydrogen Microplasma. *IEEE Transactions on Plasma Science*. 2014; 42(10): 2650–2651. [doi: 10.1109/TPS.2014.2324536](https://doi.org/10.1109/TPS.2014.2324536)
- [3] George A, Shen B, Craven M, Wang Y, Kang D, Wu C and Tu X. A Review of Non-Thermal Plasma Technology: A novel solution for CO2 conversion and utilization. *Renewable and Sustainable Energy Reviews*. 2021; 135: 109702. doi.org/10.1016/j.rser.2020.109702
- [4] Corbella C, Portal S, Lin L and Keidar M. Non-thermal plasma multi-jet platform based on a flexible matrix. *Review of Scientific Instruments*. 2021; 92(8): 083505. doi.org/10.1063/5.0057438
- [5] Zhou R, Wang X, Zhou R, Weerasinghe J, Zhang T, Xin Y, ... Ostrikov K. Non-thermal plasma enhances performances of biochar in wastewater treatment and energy storage applications. *Front. Chem. Sci. Eng*. 2021. doi.org/10.1007/s11705-021-2070-x
- [6] Mohamed H, GebSKI E, Reyes R, Beane S, Wigdahl B, Krebs F.C, Stapelmann K and

- Miller V. Differential Effect of Non-Thermal Plasma RONS on Two Human Leukemic Cell Populations. *Cancers*. 2021; 13(10): 2437.
doi.org/10.3390/cancers13102437
- [7] Lin A, Razzokov J, Verswyvel H, Privat-Maldonado A, De Backer J, Yusupov M, Cardenas De La Hoz E, Ponsaerts P, Smits E and Bogaerts A. Oxidation of Innate Immune Checkpoint CD47 on Cancer Cells with Non-Thermal Plasma. *Cancers*. 2021; 13(3): 579.
doi.org/10.3390/cancers13030579
- [8] Khabipov A, Freund E, Liedtke K.R, Käding A, Riese J, van der Linde J, Kersting S, Patrick L and Bekeschus S. Murine Macrophages Modulate Their Inflammatory Profile in Response to Gas Plasma-Inactivated Pancreatic Cancer Cells. *Cancers*. 2021; 13(11): 2525.
doi.org/10.3390/cancers13112525
- [9] Gao H, Wang G, Chen B, Zhang Y, Liu D, Lu X.P, He G and Ostrikov K. Atmospheric-pressure non-equilibrium plasmas for effective abatement of pathogenic biological aerosols, *Plasma Sources Sci. Technol.* 2021; 30(5): 053001.
doi.org/10.1088/1361-6595/abf51b
- [10] Bruggeman P, Iza F and Brandenburg R. Foundations of atmospheric pressure non-equilibrium plasmas. *Plasma Sources Science and Technology Plasma Sources Sci. Technol.* 2017; 26(12): 123002.
doi.org/10.1088/1361-6595/aa97af
- [11] Kunhardt E. Generation of large-volume, atmospheric-pressure, nonequilibrium plasmas. *IEEE Trans. Plasma Sci.* 2000; 28(1): 189–200.
[doi:10.1109/27.842901](https://doi.org/10.1109/27.842901)
- [12] Mathew D, Bastiaens H, Boller K and Peters P. Effect of preionization, fluorine concentration, and current density on the discharge uniformity in F2 excimer laser gas mixtures. *J. Appl. Phys.* 2007; 102 (3): 033305.
doi.org/10.1063/1.2767869
- [13] Aldea E, Peeters P, De Vries H and Van De Sanden. Atmospheric glow stabilization. do we need pre-ionization?. *Surf. Coat. Technol.* 2005; 200(1–4): 46–50.
doi.org/10.1016/j.surfcoat.2005.01.052
- [14] Laroussi M, Alexeff I, Richardson J and Dyer F. The resistive barrier discharge. *IEEE Trans. Plasma Sci.* 2002; 30 (1, Part 1): 158–159.
[doi: 10.1109/TPS.2002.1003972](https://doi.org/10.1109/TPS.2002.1003972)
- [15] Andre P, Barinov Y, Faure G, Kaplan V, Lefort A, Shkol S and Vacher D. Experimental study of discharge with liquid non-metallic (tap-water) electrodes in air at atmospheric pressure. *J. Phys. D: Appl. Phys.* 2001; 34 (24): 3456–3465.
doi.org/10.1088/0022-3727/34/24/306
- [16] Lu X and Laroussi M. Atmospheric pressure glow discharge in air using a water electrode. *IEEE Trans. Plasma Sci.* 2005; 33 (2, Part 1): 272–273. [doi:10.1109/TPS.2005.844946](https://doi.org/10.1109/TPS.2005.844946)
- [17] Bruggeman P, Ribezl E, Maslani A, Degroote J, Malesevic A, Rego R, Vierendeels J and Leys C. Characteristics of atmospheric pressure air discharges with a liquid cathode and a metal anode. *Plasma Sources Sci. Technol.* 2008; 17 (2): 025012. doi.org/10.1088/0963-0252/17/2/025012
- [18] Staack D, Farouk B, Gutsol A.F and Fridman A. Spatially resolved temperature measurements of atmospheric-pressure normal glow microplasmas in air. *IEEE Trans. Plasma Sci.* 2007; 35(5, Part 2): 1448–1455. [doi: 10.1109/TPS.2007.904959](https://doi.org/10.1109/TPS.2007.904959)
- [19] Akishev Y, Goossens O, Callebaut T, Leys C, Napartovich A and Trushkin N. The influence of electrode geometry and gas flow on corona-to-glow and glow-to-spark threshold currents in air. *Journal of Physics D: Applied Physics.* 2001; 34(18): 2875–2882.
doi.org/10.1088/0022-3727/34/18/322
- [20] Akishev Y, Goossens O, Callebaut T, Leys C, Napartovich A and Trushkin N. The DC glow discharge at atmospheric pressure. *IEEE Transactions on Plasma Science.* 2002; 30(1): 176–177. [doi: 10.1109/TPS.2002.1003981](https://doi.org/10.1109/TPS.2002.1003981)
- [21] Staack D, Farouk B, Gutsol A.F and Fridman A. Stabilization of the ionization overheating thermal instability in atmospheric pressure microplasmas. *Journal of Applied Physics.*

- 2009; 106(1): 013303.
doi.org/10.1063/1.3143781
- [22] Moss M S, Yanallah K, Allen R W K and Pontiga, F. An investigation of CO₂ splitting using nanosecond pulsed corona discharge: effect of argon addition on CO₂ conversion and energy efficiency. *Plasma Sources Science and Technology*.2017; 26(3): 035009.
doi.org/10.1088/1361-6595/aa5b1d
- [23] Scally L, Gulan M, Weigang L, Cullen P and Milosavljevic V. Significance of a Non-Thermal Plasma Treatment on LDPE Biodegradation with *Pseudomonas Aeruginosa*. *Materials*. 2018; 11(10): 1925.
doi.org/10.3390/ma11101925
- [24] Shaojun Xu, Pericles I K, Philip A M and Christopher W. CO₂ dissociation in a packed-bed plasma reactor: effects of operating conditions. *Plasma Sources Sci. Technol.*2018; 27(7): 075009
doi.org/10.1088/1361-6595/aacd6a
- [25] Galeev I G and Asadullin T Ya. Improving of stability of the volumetric glow discharge in the gas flow. *Journal of Physics: Conference Series*.2017; 789: 012012.
doi.org/10.1088/1742-6596/789/1/012012
- [26] Morgan N and ElSabbagh M. Hydrogen Production from Methane Through Pulsed DC Plasma. *Plasma Chem Plasma Process*.2017; 37(5): 1375–1392.
doi.org/10.1007/s11090-017-9829-3
- [27] Sasaki K, Hosoda R and Shirai N. Negative ion species in atmospheric-pressure helium dc glow discharge produced in ambient air. *Plasma Sources Sci*.2020; 29(8): 085012.
doi.org/10.1088/1361-6595/aba6a3
- [28] Országh J, Danko M, Ribar A and Matejčík Š. Nitrogen second positive system studied by electron-induced fluorescence. *Nuclear Instruments and Methods in Physics Research Section B: Beam Interactions with Materials and Atoms*.2012; 279: 76–79.
doi.org/10.1016/j.nimb.2011.10.031
- [29] Brooks C. *Weather Elements*. Nature.1942; 150: 728–729. doi.org/10.1038/150728a0
- [30] B S. Ozone developed by Humidity and Electricity. *Nature*.1870; 2: 473–474.
doi.org/10.1038/002473b0
- [31] Torben D, Nripen D, Paul A, Rhiannon M. C, Christopher J. H, Robert B, Naresh P, Bao Y, Ali Z, Samuel J, Kyle J, Jian Z, Michael S and Kouros K. Surface Water Dependent Properties of Sulfur-Rich Molybdenum Sulfides: Electrolyteless Gas Phase Water Splitting. *ACS Nano*. 2017; 11(7): 6782–6794.
doi.org/10.1021/acsnano.7b01632
- [32] Hafizi B, Palastro J, Peñano J, Jones T, Johnson L, Helle M, Kaganovich D, Chen Y and Stamm A. Stimulated Raman and Brillouin scattering, nonlinear focusing, thermal blooming, and optical breakdown of a laser beam propagating in water. *Journal of the Optical Society of America B*. 2016; 33(10): 2062-2072.
doi.org/10.1364/JOSAB.33.002062
- [33] Meichsner J, Schmidt M, Schneider R and Wagner E.__(Eds.). *Nonthermal Plasma Chemistry and Physics* (1st ed.). CRC Press.2013.
doi.org/10.1201/b12956
- [34] Bruggeman P, Ribižl E, Maslani A, Degroote J, Malesevic A, Rego R, Vierendeels J and Christophe L. Characteristics of atmospheric pressure air discharges with a liquid cathode and a metal anode. *Plasma Sources Science and Technology*. 2008; 17(2): 025012.
doi.org/10.1088/0963-0252/17/2/025012
- [35] NIST Atomic Spectra Database. Available from:
https://physics.nist.gov/PhysRefData/ASD/lines_form.html
- [36] Machala Z, Janda M, Hensel K, Jedlovský I, Leštinská L, Foltin V, Martišovítš V and Morvová M. Emission spectroscopy of atmospheric pressure plasmas for biomedical and environmental applications, *Journal of Molecular Spectroscopy*.2007; 243(2): 194-201.
doi.org/10.1016/j.jms.2007.03.001
- [37] Aldea E Private communications.
- [38] Cong, Li, Zhang J, Yao Z, Xingwei W, Chenfei Z and Hongbin D. Diagnosis of

Electron, Vibrational and Rotational Temperatures in an Ar/N₂ Shock Plasma Jet Produced by a Low-Pressure DC Cascade Arc Discharge. *Plasma Sci. Technol.*2013; 15(9): 875.

doi.org/10.1088/1009-0630/15/9/08

[39] Jing Y, Yanan Y, Jingbo L and Bailiang P. Modeling of a diode transverse-pumped cesium vapor laser. *Appl. Phys. B.* 2014; 115(4): 571–576. doi.org/10.1007/s00340-013-5638-4

[40] HR Griem. *Spectra Line Broadening in Plasmas.* 1st ed. New York: Academic Press; 1974.

[41] Gigosos M and Cardeñoso V. New plasma diagnosis tables of hydrogen Stark broadening including ion dynamics. *Journal of Physics B: Atomic, Molecular and Optical Physics.*1996; 29(20): 4795–4838.

doi.org/10.1088/0953-4075/29/20/029

[42] Laux CO, Spence TG, Kruger CH and Zare RN. *Optical diagnostics of atmospheric pressure air plasmas.* 2003; 12(2): 125–138. doi.org/10.1088/0963-0252/12/2/301

[43] Kunze Hans-Joachim. *Introduction to plasma spectroscopy.* 1st ed. Berlin: Springer; 2009. doi.org/10.1007/978-3-642-02233-3

[44] Zhang, Yu, Wen X-H and Yang W-H. Excitation temperatures of atmospheric argon in dielectric barrier discharges. *Plasma Sources Science and Technology.*2007; 16(3): 441–447. doi.org/10.1088/0963-0252/16/3/003

[45] Idris N, Usmawanda TN, Lahna K and Ramli M. Temperature estimation using Boltzmann plot method of many calcium emission lines in laser-plasma produced on river clamshell sample. *J. Phys.: Conf. Ser; The 8th International Conference on Theoretical and Applied Physics;*2018 Sep 20–21; Medan, Indonesia: IOP; 2018. 1120 (1): 012098.

doi.org/10.1088/1742-6596/1120/1/012098

الملخص العربي

الخصائص الطيفية لمصدر بلازما مستقر من ابرة الي لوحه بالضغط الجوي

احمد عبدالراضي (1)، احمد سمير (2)،

فاروق الاكشر (3)، عبده جارمون (3)

منصور الصباغ (2,3)

1 الهيئة العامة للارصاد الجوية المصرية – القاهرة

2 مركز تكنولوجيا البلازما - جامعة الازهر – القاهرة

3 قسم الفيزياء-كلية العلوم بنين – جامعة الازهر – القاهرة

تم الحصول على تفريغ كهربى مستمر ومستقر لغاز الأرجون في الضغط الجوي ما بين ابرة و لوح معدنى . في هذا البحث ، تم دراسة انهيار غاز الأرجون المتدفق في الهواء كما (مصدر البلازما) بواسطة طريقة التحليل الطيفي للانبعثات الضوئية. وقد لوحظ أطياف انبعاث الأنواع المثارة من الهيدروجين الذري والنيوتروجين الجزيئي والأرجون. وتم قياس درجات الحرارة الدورانية والاهتزازية للتفريغ عن طريق مقارنة محاكاة أطياف الانبعاث الضوئي مع القياسات الطيفية من التفريغ وعن طريق استخدام عدة نطاقات اهتزازية مختلفة من النظام الموجب الثاني SPS . وكشفت الخصائص البصرية للتفريغ أن البلازما المتكونة غير متزنة وان درجة حرارة الدورانية تبلغ 1087 كلفن ودرجة حرارة الاهتزازية تبلغ 1661 كلفن. وطُبقت طريقة بولتزمان لتقدير درجة حرارة الإثارة الإلكترونية ووجد أن هي 1.36 eV و 1.1 eV للبلازما المولدة مع معدلات تدفق الأرجون من SLM1.0 و SLM 0.5 على التوالي. وأثبتت هذه النتيجة الطابع الغير متزنة للبلازما المتكونة.